Peel-off-Scanning to obtain Radial Differentiation of Fractal and Complexity Features in Cell Nuclei

Birgitte Nielsen, Fritz Albregtsen, Sivalingam Baheerathan
Department of Informatics, University of Oslo, Norway
and Håvard E. Danielsen
Division of Digital Pathology, The Norwegian Radium Hospital

Abstract

A polygonization-based method is used to estimate fractal features from digitized transmission electron micrographs (TEM) of mouse liver cell nuclei. In order to obtain separate estimates of the development of fractal features in the center and periphery of a cell nucleus during carcinogenesis, the fractal features have been estimated from 1D curves obtained by scanning the 2D cell nuclei in a spiral-like fashion called "peel-off-scanning". The peripheral part (outer 30%) of the cell nuclei contained important texture information about the differences between the classes. The classification performance of five complexity features were also enhanced when separate estimates were made in the center and periphery of the cell nuclei.

The combination of two features and two segments, one feature from the 30% peripheral part and one feature from the 70% central part of the cell nuclei, gave good classification results for the four class problem of normal, regenerating, noduli and tumor classes.

1 Introduction

Chromatin structure has traditionally been regarded as an important diagnostic clue in pathology. The chromatin structure, which reflects and partially controls genetic functions, changes within cell nuclei as cancer develops. In routine practice the changes in cell nuclei are assessed subjectively and are used in diagnosis and grading of malignancies. Quantification of such changes may therefore be a diagnostic aid, and may also contribute towards a further understanding of the biological processes involved.

Fractal geometry is well suited to quantify the complexity of both disordered patterns and complex deterministic structures. Even for structures that are not true mathematical fractals, we may obtain a simple quantification of the complexity over the range of scales there the phenomenon *behaves* like a fractal.

Despite an increasing interest in using fractals in biology and medicine, particularly to describe single cells [21], [26], [7], [15], [23], [5], most studies of fractal features of cells are only considering fractal descriptions of the curve outlining the cell contour in binary images, and are almost exclusively using only the fractal dimension [13], [16], [3], [20]. Only a few studies [17], [10], [19] have utilized fractal geometry to characterize the chromatin structure in gray level images of the cell nuclei.

In order to obtain separate estimates of the development of fractal features in the center and periphery of a cell nucleus during carcinogenesis, Nielsen et al. [19] transformed 2D gray level images of liver cell nuclei into 1D gray level signals by scanning the cell nuclei in a spiral-like fashion called "peel-off-scanning". When quantifying the amount and arrangement of chromatin close to the nuclear membrane, the "peel-off-scanning" seems indispensable, as it is very hard to achieve a separate treatment of center and periphery using fixed 2D windows or other arrangements based on the principal orthogonal directions of the image.

A 1D polygonization-based method [1] was then used to estimate several fractal texture features in different segments of the 1D gray level curves obtained. It was found that when dividing the cell nuclei into 10 segments, the second 10% peripheral segment gave the best classification results. However, the outer 25-30% of the nuclei contained most of the *fractal* textural information about the differences between the classes, while it was necessary to include one Gray Level Cooccurrence Matrix (GLCM) feature [4] from the central part to discriminate between all classes.

The aim of the present work was therefore 1) to investigate a more robust and simplified classification scheme based on the peripheral 30% and the central 70% of the cell nuclei, 2) to quantify the relation between fractal features and first order complexity features [2] which give a second order description of 2D image texture. We will also discuss the merits of a) obtaining these features from 1D curves obtained by "peel-off-scanning", b) a 2D treatment of the segments outlined by the "peel-off-scanning", and c) obtaining the features from the whole cell nucleus.

2 Material and Methods

2.1 Data Description

Care and treatment of animals, preparation of liver specimens, and preparation of liver sections are described in [19]. The first group was a normal (non-proliferating) control group and consisted of liver samples from five animals. The second (regenerating) group contained normal, but proliferating cells, and included liver samples from five animals. The third (premalignant) group consisted of a total of 15 nodules (0.5-2 mm in diameter) isolated by liver perfusion of 15 mice. For analysis of hepatocellular carcinomas (fourth group), one well defined tumor was taken randomly from the liver of each of 11 animals. The value of each texture feature used here to classify each sample (lesion) was the mean value of about 100 cell nuclei from each sample.

In the following, the four classes will be designated by the letters N (normal), R (regenerating), P (premalignant) and T (tumor).

Ultrathin liver sections (approximate thickness=60-90 nm) were studied at a magnification of 2500 in a JEOL EX1200 transmission electron microscope at 60kv with a $20\mu m$ aperture. The cell images were recorded on Kodak 4489 EM photographic film and were examined using a Kontron (Germany) Image Processing System (IBAS), in which a Sony CCD video camera (XC-77CE, Japan) was used to capture the electron micrographs. The images of cell nuclei were selected at random from a larger set of cell images from each lesion. Each nuclear image was stored in $512 \times 512 \times 8$ bits, and the pixel resolution was 39 nm per pixel on the cell specimen.

A 3×3 median filter was applied in order to reduce possible noise without too much unwanted altering of the local texture. This was followed by a manual segmentation to extract the cell nucleus as the region of interest. Subsequently, the histograms of all images were normalized to the same mean value (127.5) and standard deviation (50.0). The gray level value 255 was used as background.

2.2 Spiral Scanning

As described in [19], a backtracking bug follower has been used as a spiral scanning algorithm. Starting with the segmented cell nucleus, we follow the (outer) contour of the nucleus, and spiral inwards as we peel off layer by layer of pixels from the nucleus, forming a 1D gray level signal.

The 1D gray level signal resulting from the "peel-off-scanning" of each cell nucleus was divided into a peripheral 30% and a central 70% segment. Figure 1 shows examples of cell nuclei from each class, together with the mean gray level histograms from periphery and center for each of the four classes.

2.3 1D Fractal Features

2.3.1 Fractal Dimension

An estimate of the fractal dimension of a 2D gray level surface is usually obtained by counting the number of boxes of different sizes that are needed to cover the surface. A number of refinements of this scheme exist [24], [12], [22], [8].

For 1D signals such as those obtained by our scanning procedure, several algorithms are applicable to the problem of measuring the length of an irregular curve. Mandelbrot [18] suggested walking a yardstick of length ϵ along the curve. This *constant-length* method is not even theoretically exact for curves without self-similarity, and yields poor results if the curve contains only a small number of points. Thus, a *variable-length* method should be used.

Our method for estimation of fractal dimension from such 1D curves [1] is based on the polygonization method of Wall and Danielsson [25]. This method steps from point to point through an ordered sequence of points, and outputs the previous point as a new break point if the area deviation per unit length of the approximating line segment exceeds a prespecified tolerance, $T(\kappa)$.

We approximate the 1D gray level signal obtained by the "peel-off-scanning" process by polygonization with several values of the tolerance, $T(\kappa)$. For each tolerance value the total length of the line segments that approximate the curve is summed up by $S(\kappa) = \sum_{j=1}^{m-1} s_j(\kappa)$.

Using the variable length polygonization concept, the upper and lower limits of the useful range of $T(\kappa)$ values may be found automatically, without visual inspection, by simple upper and lower limits on the number of line segments in a polygonization of a curve consisting of a given number of points [1], [19]. Given the range of $T(\kappa)$-values that satisfies these criteria, and the corresponding set of points in the $\{\log[T(\kappa)], \log[S(\kappa)]\}$-domain, we find the coefficients of a least-squares fitted linear relation,

$$\log[S(\kappa)] = \hat{a} + \hat{b}\log[T(\kappa)], \quad \hat{b} = \hat{H} - 1 \qquad (1)$$

as well as the uncertainty in the linear slope coefficient, and the linear correlation coefficient, $r_{T,S}$. Thus, we have an estimate of the validity of the fit as well as the uncertainty in the estimated Hurst-parameter $\hat{H}$ (fractal dimension $\hat{D} = 2 - \hat{H}$), together with the "prefactor" $\hat{a}$.

2.3.2 Lacunarity Features

Mandelbrot [18] also introduced *lacunarity*, Λ, to quantify texture. The significance of lacunarity is that it describes the deviation from homogeneity in the texture. The 2D lacunarity measures of Voss [24] and Keller *et al.* [12] are both vectors of variance measures computed from a set of distributions, each of which is obtained for a certain value of the box size. Thus, we note that lacunarity is a *vector*, with discrete values computed from separate distributions,

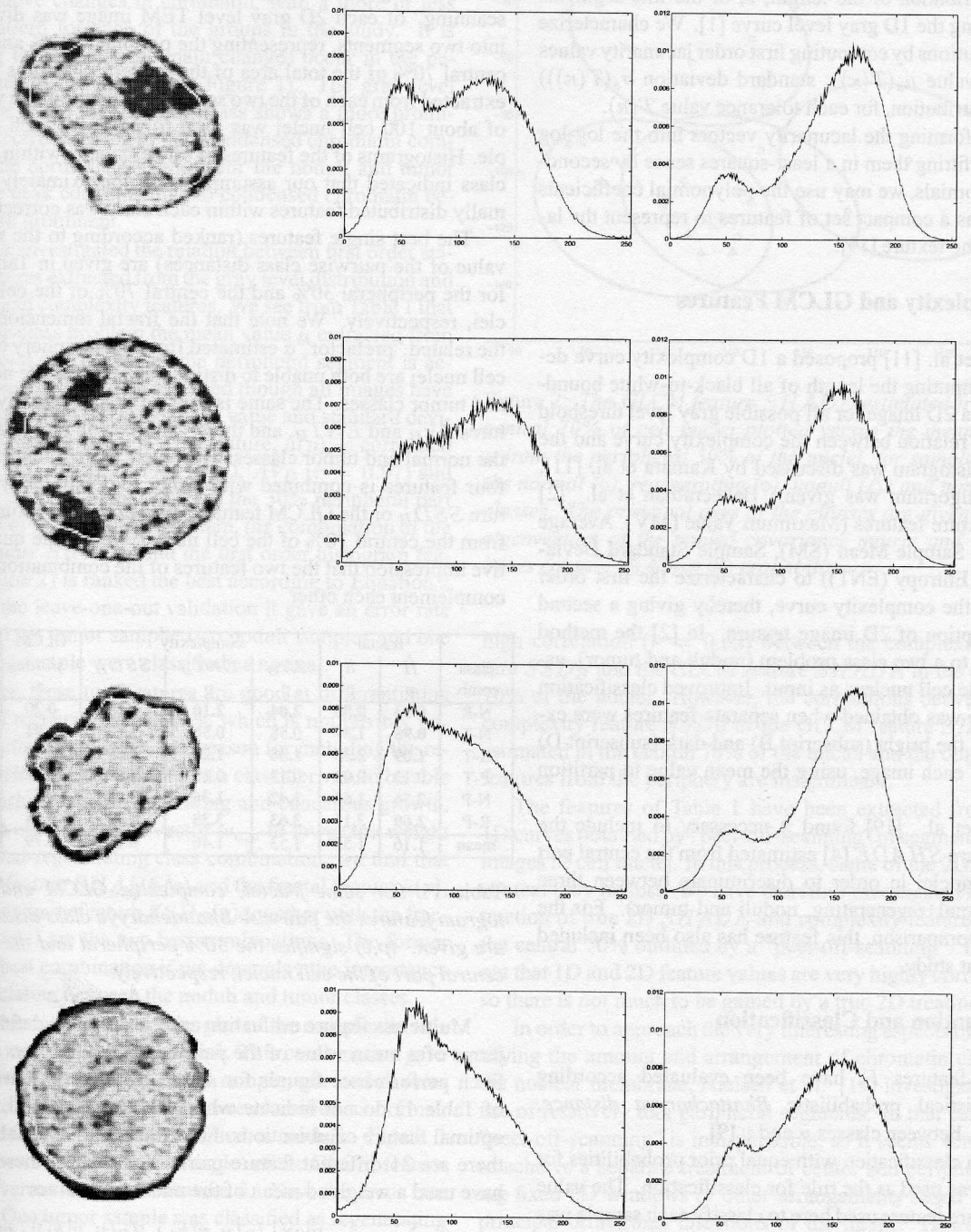

Figure 1: **First column:** *Examples of liver cell nuclei from normal, regenerating, noduli and tumor samples. The borders between the 30% peripheral and 70% central part are outlined as a thin white line.* **Second column:** *The mean gray level histograms from all cell nuclei within each of the four classes, based on the 30% peripheral part of nuclei.* **Third column:** *The mean gray level histograms from all cell nuclei within each of the four classes, based on the central 70% of the nuclei.*

while a constraining parameter is varying.

For each tolerance value $T(\kappa)$ of the polygonization we find the distribution of the length, s, of the line segments approximating the 1D gray level curve [1]. We characterize these distributions by computing first order lacunarity values (e.g. mean value $\mu_s(T(\kappa))$, standard deviation $\sigma_s(T(\kappa))$) from this distribution, for each tolerance value $T(\kappa)$.

By transforming the lacunarity vectors into the log-log domain and fitting them in a least-squares sense by second-order polynomials, we may use the polynomial coefficients α, β and γ as a compact set of features to represent the lacunarity of the texture [19].

2.4 Complexity and GLCM Features

Kamata et al. [11] proposed a 1D complexity curve defined by computing the length of all black-to-white boundaries within a 2D image for all possible gray level threshold values. The relation between the complexity curve and the gray level histogram was discussed by Kamata et al. [11], and a fast algorithm was given. Baheerathan et al. [2] used five texture features (Maximum Value (MV), Average Value (AV), Sample Mean (SM), Sample Standard Deviation (SSD), Entropy (ENT)) to characterize the first order statistics of the complexity curve, thereby giving a second order description of 2D image texture. In [2] the method was applied to a two class problem (noduli and tumor), using the whole cell nucleus as input. Improved classification performance was obtained when separate features were extracted from the bright (subscript B) and dark (subscript D) partitions of each image, using the mean value to partition the images.

Nielsen et al. [19] found it necessary to include the GLCM feature $SHADE$ [4] estimated from the central part of the cell nuclei in order to discriminate between three classes (normal+regenerating, noduli and tumor). For the purpose of comparison, this feature has also been included in the present study.

2.5 Evaluation and Classification

Texture features F_i have been evaluated according to the statistical probabilistic *Bhattacharyya distance*, $J_B(u, v|F_i)$, between classes u and v [9].

Bayesian classification with equal prior probabilities for each class was used as the rule for classification. The value of each texture feature used here to classify each sample was the mean value of about 100 cell nuclei. The feature distribution within each class was assumed to be multivariate normal and the within-class covariance matrices were assumed equal. Because of the small number of samples available, we have used the leave-one-out method to estimate the misclassification rates. Thus, the same data set was used both to define and evaluate the linear discriminant functions.

3 Results and Discussion

The 1D gray level signal resulting from the "peel-off-scanning" of each 2D gray level TEM image was divided into two segments, representing the peripheral 30% and the central 70% of the total area of the nucleus. Features were extracted from each of the two segments, and the mean value of about 100 cell nuclei was used to represent each sample. Histograms of the features of all cell nuclei within each class indicated that our assumption of approximately normally distributed features within each class was correct.

The best single features (ranked according to the mean value of the pairwise class distances) are given in Table 1, for the peripheral 30% and the central 70% of the cell nuclei, respectively. We note that the fractal dimension and the related "prefactor" $\hat{a}$ estimated from the periphery of the cell nuclei are both unable to distinguish between the noduli and tumor classes. The same is true for the complexity features AV_B and ENT_B, and these features will also confuse the normal and tumor classes. However, when one of these four features is combined with either the complexity feature SSD_B or the GLCM feature $SHADE$, both estimated from the central 70% of the cell nuclei, we get the qualitative impression that the two features of the combination will complement each other.

	fractal		complexity			GLCM	hist.
class	$\hat{H}$	$\hat{a}$	AV_B	ENT_B	SSD_B	*shade*	μ
comb.	p	p	p	p	c	c	p
N-R	0.03	**0.85**	**2.04**	**2.10**	0.38	0.20	**2.99**
N-T	**0.95**	**1.37**	0.58	0.56	**1.08**	**1.91**	0.67
R-T	**1.09**	**2.33**	**1.38**	**1.26**	0.29	0.74	**1.25**
P-T	0.13	0.03	0.13	0.15	**1.49**	**1.73**	0.11
N-P	**2.16**	**1.64**	**1.42**	**1.36**	0.04	0.02	**1.07**
R-P	**2.60**	**3.11**	**3.63**	**3.35**	0.71	0.14	**3.36**
mean	1.16	1.55	1.53	1.46	0.66	0.79	1.57

Table 1: *For some fractal, complexity, GLCM and histogram features the pairwise Bhattacharyya class distances are given. (p,c) signifies the 30% peripheral and the 70% central part of the cell nuclei, respectively.*

Multiclass feature evaluation criteria are often defined in terms of a mean value of the pairwise class distances [14]. Such performance figures for single features (bottom row of Table 1) do not indicate which features that will form optimal feature combinations. For the 7 features of Table 1, there are 21 different feature pairs. For each of these, we have used a weighted mean of the maximum values

$$V_{k,l} = \frac{\sum_{u,v;u\neq v} \max\left[J_B(u,v|F_k), J_B(u,v|F_l)\right] \cdot w_{u,v}}{\sum_{u,v;u\neq v} w_{u,v}} \tag{2}$$

in a quantitative ranking of the pairwise combinations of two features F_k and F_l. The weight vector $w_{u,v}$ covers all the six pairwise class combinations, allowing us to vary the relative importance of correct classifications between classes.

Danielsen [6] found that the mean gray level distribution of all cell nuclei in each class showed both quantitative and qualitative changes in chromatin, with a more or less distinct pattern for each of the groups in the study. It is interesting to note that the main changes occur in the peripheral part of the nuclei (see Figure 1). The gray level distribution of the regenerating class shows a more prominent peak corresponding to non-condensed chromatin compared to the normal class, while for the noduli and tumor classes the peak corresponding to condensed chromatin becomes more prominent.

We have investigated the relation between first order statistical features extracted from the gray level distribution and the fractal and complexity features. We see from Table 1 that for the four-class problem the mean value μ extracted from the gray level distribution of the peripheral segment is actually among the best features, even though all images have been normalized to the same mean value and standard deviation during preprocessing. This feature, $\mu(p)$, is correlated with $\hat{H}$ ($r = -0.82$), $\hat{a}$ ($r = 0.84$), AV_B ($r = 0.97$) and ENT_B ($r = 0.96$) extracted from the 30% peripheral part of nuclei. For the four class problem, the combination of the GLCM feature $SHADE$ and the first order histogram feature μ (Figure 2) is ranked the best according to Equation 2 above. In the leave-one-out validation it gave an error rate of 11.1%. One tumor sample, two noduli samples and one regenerating sample were classified as normal.

However, these two features are good at differentiating normal and regenerating samples, which is not terribly important in clinical practice. The reason for including the regenerating class was to ensure that a classifier would be able to distinguish between regenerating and cancerous growth. Thus, if we use the weight vector $w_{u,v}$ to lower the weight of the normal-regenerating class combination, we find that the GLCM feature $SHADE(c)$ and the fractal feature $\hat{a}(p)$, and the complexity feature $SSD_B(c)$ together with the fractal feature $\hat{a}(p)$ are the two best combinations. The former is also the best combination if we downplay the importance of differenciating between the noduli and tumor classes.

Figure 3 (top) shows a scatter plot of the complexity feature SSD_B and the fractal feature $\hat{a}$. This combination gave an error rate of 11.1%. One tumor sample, one noduli sample and one regenerating sample was classified as normal, and one tumor sample was classified as noduli. Figure 3 (bottom) shows the similar scatter plot of the GLCM feature $SHADE$ versus the fractal feature $\hat{a}$. Now the error rate was 8.3%. One tumor sample was classified as regenerating and one noduli and one regenerating sample was classified as normal. This demonstrates that the classification performance of the two feature combinations are approximately equivalent.

In the peripheral part of the nuclei, the two fractal features are obviously correlated ($r = -0.89$), and so are the two best complexity features ($r = 0.99$). There is also a high correlation ($r = 0.93$) between the complexity feature SSD_B and the GLCM feature $SHADE$ in the central 70% of the nuclei. However, the correlations between the complexity feature SSD_B or the GLCM feature $SHADE$ estimated in the central 70% of the nuclei and the other four features from the periphery are insignificant.

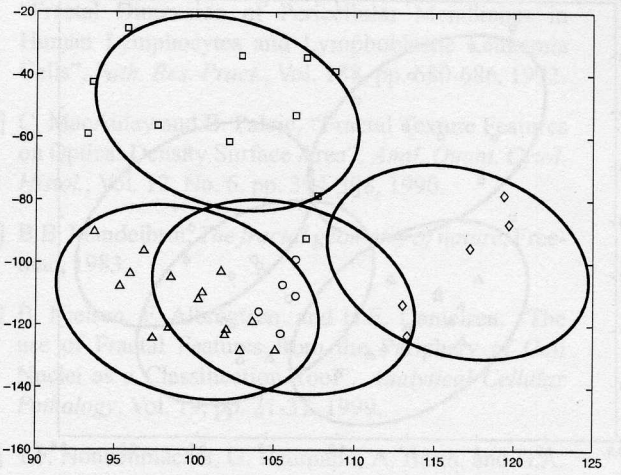

Figure 2: *The GLCM feature $SHADE$ estimated from the central 70% of cell nuclei plotted versus the mean value μ from the peripheral 30% of the nuclei, for samples from the normal (○), regenerating (◇), noduli (△) and tumor (□) classes. The principal axes of the ellipses are given by the eigenvectors of the pooled covariance matrix and the ellipses contain 95.4% of the probability.*

The features of Table 1 have been extracted from the 1D curves obtained by "peel-off-scanning" of segmented 2D images of cell nuclei. In this process, some of the 2D image context may be lost. We have therefore investigated the extraction of true 2D $SHADE$ and complexity features from the central 70% outlined by a "peel-off-scanning". It turns out that 1D and 2D feature values are very highly correlated, so there is not much to be gained by a true 2D treatment.

In order to approach the very interesting aspects of quantifying the amount and arrangement of chromatin close to the nuclear membrane, Nielsen et al. [19] investigated the use of relatively thin peripheral segments. In that case, the "peel-off-scanning" is indispensable, as it seems very hard to acheive a separate treatment of center and periphery using fixed 2D windows or other arrangements based on the principal orthogonal directions of the image. However, a 1D treatment based on "peel-off-scanning" in the periphery may be combined with a 2D treatment of the central part of the cell nucleus. This may be relevant for the lower resolution images from light microscopy.

There are no significant correlations between the same features estimated in the center and periphery, or the same complexity feature estimated in the bright and dark partition

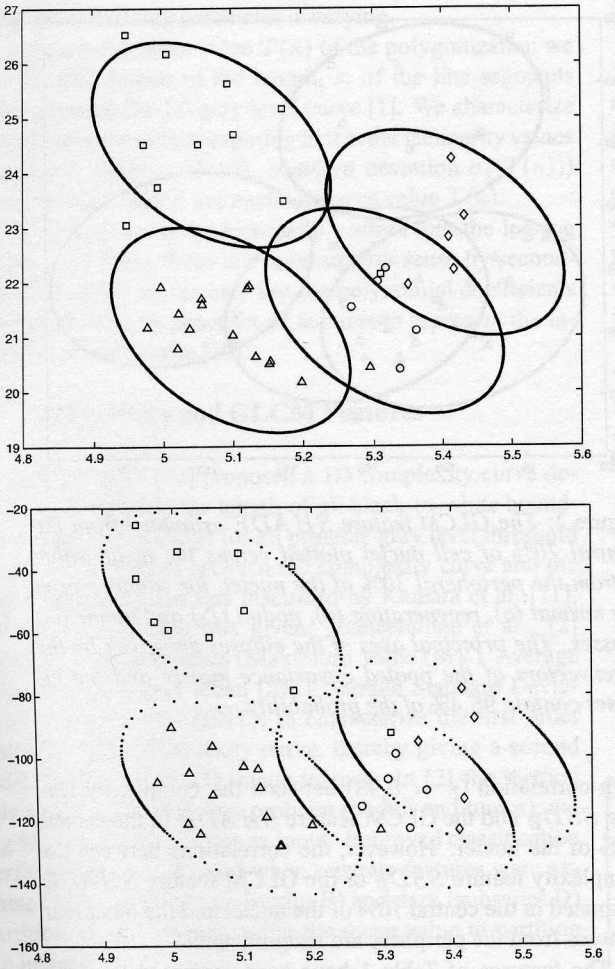

Figure 3: *The complexity feature SSD_B (top) and the GLCM feature $SHADE$ (bottom) estimated from the central 70% of cell nuclei plotted versus the fractal feature $\hat{a}$ as obtained by the 1D polygonization method from the peripheral 30% of nuclei, for samples from the normal (○), regenerating (◇), noduli (△) and tumor (□) classes. The principal axes of the ellipses are given by the eigenvectors of the pooled covariance matrix and the ellipses contain 95.4% of the probability.*

of the image. This confirms the finding of Nielsen et al. [19] that the previous implicit assumption of a stationary nuclear texture is suboptimal, and that a number of texture features benefit from being applied separately to the peripheral and central parts of the cell nuclei.

We find a significant quantitative decrease in the estimated fractal dimension of the peripheral part of the cell nuclei from the normal/regenerating classes to the noduli/tumor classes. This confirms the qualitative visual impression that the peripheral condensations of heterochromatin are larger in the latter two classes, making the gray level surface structures less complex.

We note that the (dark) nucleoli are randomly present in some of the nuclear images, and that these have not been removed by segmentation. Thus, they may influence the parameters extracted from each single cell. However, as the value of each texture feature used here to classify each sample (lesion) is the mean of about 100 cell nuclei, this should not bias the results, unless the probability of nucleoli occurring in the two segments differ significantly between the classes.

It is evident from Figures 2 and 3 that in the present case, the assumption of equal within-class covariance matrices may not be optimal. This may to some extent have influenced the classification results. However, given the limited size of the data set, it would not be possible to estimate separate covariance matrices for each class and still retain the necessary statistical confidence.

Work is in progress on testing the methods presented here on a different set of clinical data from light microscopy. When working with large volumes of cells, a (semi)-automatic segmentation of cell nuclei will be advantageous, as it both reduces the uncertainty caused by manual segmentation and ensures the reproducibility of the results.

In conclusion, we have shown that the robust and simplified classification based on one fractal feature from the peripheral 30% and either a complexity or a GLCM feature from the central 70% of the cell nuclei, give good classification results for the four class problem of TEM images of liver cell nuclei.

Acknowledgments

We thank Ruth Puntervold and the late Barbara Schuler of the Division of Digital Pathology, the Norwegian Radium Hospital, for their skillful technical assistance. We also thank Professor Knut Liestøl for useful comments.

References

[1] F. Albregtsen and B. Nielsen, "Fractal Dimension and Lacunarity Estimated by Sequential 1D Polygonization of 2D Images", in: *Theory and Applications of Image Analysis II* - Selected papers from the 9th Scandinavian Conference on Image Analysis, G. Borgefors (ed.), World Scientific Publ Co, pp. 79-88, 1995.

[2] S. Baheerathan, F. Albregtsen, and H.E. Danielsen, "New texture features based on the complexity curve", *Pattern Recognition*, Vol. 32, No. 4, pp. 605-618, 1999.

[3] G. Baumann, A. Barth, and T.F. Nonnenmacher, "Measuring fractal dimensions of cell contours: practical

approaches and their limitations", in: *Fractals in Biology and Medicine*, T.F. Nonnenmacher, G.A. Losa, E.R. Weibel (eds), Birkhäuser-Verlag, Basel, pp. 182-189, 1994.

[4] R.W. Conners, M.M. Trivedi, and C.A. Harlow, "Segmentation of a High-Resolution Urban Scene Using Texture Operators", *CVGIP*, Vol. 25, pp. 273-310, 1984.

[5] S.S. Cross, "Fractals in Pathology", *Journal of Pathology*, Vol. 182, pp. 1-8, 1997.

[6] H.E. Danielsen, "Premalignant Changes in DNA Organization in Mouse Liver after Diethylnitrosamine Treatment", *Thesis*, The Norwegian Radiumhospital and Institute for Cancer Research, Oslo, Norway, ISBN 82-7633-016-9, 1991.

[7] A. Doudkine, C. MacAulay, N. Poulin, and B. Palcic, "Nuclear texture measurements in image cytometry", *Pathologica*, Vol. 87, pp. 286-299, 1995.

[8] J. Feng, W-C. Lin, and C-T. Chen, "Fractional Box-Counting Approach to Fractal Dimension Estimation", *Proc. of ICPR'96*, Vol. II, pp. 854-858, Vienna, Austria, 1996.

[9] D.J. Hand, *Discrimination and Classification*, Wiley, 1981.

[10] T. Irinopoulou, J.P. Rigaut, and M.C. Benson, "Toward Objective Prognostic Grading of Prostatic Carcinoma Using Image Analysis", *Anal. Quant. Cytol. Histol.*, Vol. 15, pp. 341-344, 1993.

[11] S. Kamata, R.O. Eason, and K. Kawaguchi, "Complexity curves versus histograms and their application to image segmentation", *Proc. of 7th Scandinavian Conf. on Image Analysis*, pp. 1070-1077, 1991.

[12] J.M. Keller, S. Chen, and R.M. Crownover, "Texture Description and Segmentation through Fractal Geometry", *CVGIP*, Vol. 45, pp. 150-166, 1989.

[13] K.M.W. Keough, P. Hyam, D.A. Pink, and B. Quinn, "Cell surfaces and fractal dimensions", *Journal of Microscopy*, Vol. 163, pp. 95-99, 1989.

[14] J. Kittler, "Feature Selection and Extraction", in K-S. Fu (ed.) *Handbook of Pattern Recognition and Image Processing*, pp. 59-83, Academic Press, 1986.

[15] G.A. Losa and T.F. Nonnenmacher, "Self-Similarity and Fractal Irregularity in Pathologic Tissues", *Mod Pathol*, Vol. 9, No. 3, pp. 174-182, 1996.

[16] G.A. Losa, B. Baumann, and T.F. Nonnenmacher, "Fractal Dimension of Pericellular Membranes in Human Lymphocytes and Lymphoblastic Leukemia Cells", *Path. Res. Pract.*, Vol. 188, pp. 680-686, 1992.

[17] C. MacAulay and B. Palcic, "Fractal Texture Features on Optical Density Surface Area", *Anal. Quant. Cytol. Histol.*, Vol. 12, No. 6, pp. 394-398, 1990.

[18] B.B. Mandelbrot, *The fractal geometry of nature*, Freeman, 1983.

[19] B. Nielsen, F. Albregtsen, and H.E. Danielsen, "The use of Fractal Features from the Periphery of Cell Nuclei as a Classification Tool", *Analytical Cellular Pathology*, Vol. 19, pp. 21-37, 1999.

[20] T.F. Nonnenmacher, G. Baumann, A. Barth, and G.A. Losa, "Digital image analysis of self-similar cell profiles", Intern. Journ. of *Bio-Medical Comp.*, Vol. 37, pp. 131-138, 1994.

[21] D. Paumgartner, G. Losa, and E.R. Weibel, "Resolution effect on the stereological estimation of surface and volume and its interpretation in terms of fractal dimensions", *Journal of Microscopy*, Vol. 121, pp. 51-63, 1980.

[22] N. Sarkar and B.B. Chaudhuri, "An Efficient Differential Box-Counting Approach to Compute Fractal Dimension of Image", *IEEE Trans. on Systems, Man and Cybernetics*, Vol. 24, pp. 115-120, 1994.

[23] T.G. Smith, G.D. Lange, and W.B. Marks, "Fractal methods and results in cellular morphology - dimensions, lacunarity and multifractals", *Journal of Neuroscience Methods*, Vol. 69, pp. 123-136, 1996.

[24] R. Voss, "Random fractals: Characterization and Measurement", in: *Scaling Phenomena in Disordered Systems*, R. Pynn and A. Skjeltorp (eds.), Plenum Press, New York, pp. 1-11, 1985.

[25] K. Wall and P.E. Danielsson, "A Fast Sequential Method for Polygonal Approximation of Digitized Curves", *CVGIP*, Vol. 28, pp. 220-227, 1984.

[26] E.R. Weibel, "Fractal geometry: a design principle for living organisms", *American Journal of Physiology*, Vol. 261, L361-L369, 1991.